Dynamics of Partial Space Elevator with Parallel Tethers and Multiple Climbers

Gangqiang Li and Zheng H. Zhu *

Department of Mechanical Engineering, York University

4700 Keele Street, Toronto, Ontario, M3J 1P3, Canada

Abstract: This paper proposes a novel concept of partial space elevator with parallel tethers and multiple climbers. The parallel tethers impacting on the dynamic response of partial space elevator is investigated based on a high fidelity and accurate model of PSE. The model is developed based on the nodal position finite element method in the arbitrary Lagrangian-Eulerian description. The results show the tethers collides when the transient motion of climbers is not the same, such as the movement direction of climbers is opposite and the time delay between climbers. It also found that the multiple climbers of each other may aggravate the libration motion of PSE without predesigned time shift. The results show the trajectories of climber very important and should be well designed to avoid the collision of tethers and assure the safety operation of load transfer.

Keyword: partial space elevator; nodal position finite element method; arbitrary Lagrangian-Eulerian; parallel tethers; multiple climbers; variable-length element.

* Corresponding Author, Tel. : + 1 416 736 2100 x 77729, fax: +1 416 736 5817. Email address: gzhu@yorku.ca.

I. Introduction

Partial Space Elevator (PSE) is an attractive alternative to the classical space elevator due to its ability for long-range transfer of payloads between two satellites at low cost [1, 2]. PSE has been a good demonstration for space elevator technology, and the construction of a PSE is relatively easy to achieve in near term [3].

Past decades have witnessed many efforts to the dynamics of PSE, and they can be categorized in terms of number of climbers, one climber case and multiple climbers. For the case of one climber, Lorenzini [4, 5] initially proposed the concept of space elevator system attached to International Space Station and study its dynamics based on the two-piece dumbbell model. Later, the transient motion of climber impacting on the dynamics of PSE is investigated [6-8], and the study of system parameters of PSE, such as mass ratio of climber to satellite, tether length, and climber's speed, influence on the dynamic characteristics of PSE is conducted. After that, the trajectory of climber is optimized to maximize the suppression of the libration angle of PSE based on the two dumbbell model [9, 10], and the feasibility study of the trajectory of climber applied to the PSE with flexible tether is conducted [10]. Recently, a stabilization method is proposed to suppress libration motion of PSE by cancelling the generated Coriolis force of moving climber though the regulation of deployment/retrieval speed at end satellites [11]. Here, just name a few, the detailed review of the dynamics of PSE with one climber can be found in our previous work [12, 13]. For the case of multiple climbers, the concept of multiple climbers with proper phase shift is proposed to alleviate the residual libration of PSE by one climber [2]. The background mechanism is that the induced Coriolis force of one moving climber is cancelled by another climber with pre-planned trajectory. From this viewpoint, the simultaneous operation of dual climbers impacting on the dynamic response of PSE is investigated, where one climber moves from bottom to upper and the other one

moves from upper to bottom [14]. The results show the simultaneously operation of two climber provide positive effect in suppressing the libration of PSE. Furthermore, different moving patterns of multiple climbers are detailed investigated [15]. To suppress the libration of PSE with multiple climbers, the concept of optimization of middle climber relative to the other climbers is firstly proposed, and the results show it is feasible.

In current paper, to take the advantage of multiple climbers and increase the efficiency of payload transfer, a novel concept of PSE with parallel tethers and multiple climber is proposed. Among it, the parallel tethers are connected by a transverse support structure with large rigidity at end satellites, and multiple climbers are supposed to operate along each tether. The transient motion of climber impacting on the libration motion of PSE is investigated by a high-fidelity model of PSE based on the nodal position finite element method.

II. Mathematical formulation of partial space elevator

A. Coordinate systems

Consider a PSE with parallel tethers moving in an arbitrary orbit initially in a central gravity field as shown in Fig. 1. The PSE consists of main satellites, sub satellites, multiple parallel elastic and flexible tethers connecting these satellites, and multiple climbers are moving up and down along the tether. For simplicity, the numbering of tether is counted from left to right, and the movement direction of climbers (in the case of multiple climbers) belong to the same tether are supposed to be the same. The satellites and climber are modeled as lumped masses with their attitude dynamics ignored, given the extremely large ratio of tether length over the dimensions of satellites and climber. The motion of the PSE is described by three sets of coordinate systems: the global inertial

frame (*OXYZ*), the local frame of element (*otbn*) and the orbital frame ($O'X_oY_oZ_o$). The detail definition of these coordinate systems can be found in our previous works [10, 12, 13].

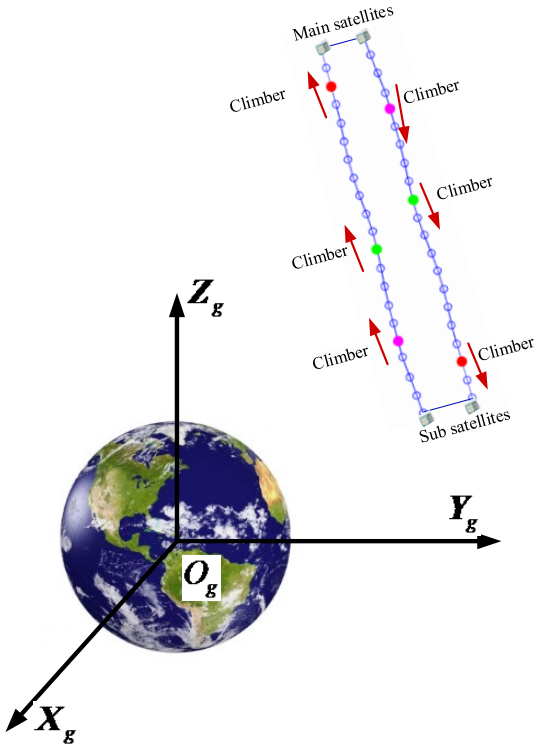

Fig. 1 Schematic of PSE with parallel tethers (two tethers) and multiple climbers.

B. Nodal Position Finite Element Formulation of Partial Space Elevator

1. Nodal position finite element formulation in ALE description

In current paper, the nodal position finite element method is used to describe tether dynamics with large rotation and displacement [16-18]. Here, to easily describe and incorporate the motion of multiple climber[13] and tether deployment or retrieval [12], the material coordinate is introduced. Thus, the position and material coordinates are together taken as the state variables of PSE. The equation of motion of PSE are derived based on the generalized D'Alembert principle [17-20]. Taking *k-th* element as an example, such that,

$$\boldsymbol{M}_{e,k}\ddot{\quad}_{,k}+\boldsymbol{F}_{g,k}-\boldsymbol{F}_{p,k} \tag{1}$$

where subscript k denotes the k-th element. $\boldsymbol{M}_e$ is the element's mass matrix, $\ddot{}$ is the vector of acceleration, $\boldsymbol{F}_e$, $\boldsymbol{F}_g$, and $\boldsymbol{F}_p$ are the vectors of elastic force, gravitational force, and the induced force due to variation of material coordinate.

After the obtaining of the equation of motion of one element, the equation of motion of PSE can be assembled together in the conventional finite element.

$$\boldsymbol{M}_e \ddot{} \quad \vdash \boldsymbol{F}_g - \boldsymbol{F}_p \tag{2}$$

where $\boldsymbol{M}_e$ is a hybrid mass matrix with satellites and climbers are supposed as lumped masses adding into the mass matrix of tether. The gravity of lumped masses is also added into the vector of gravity of tether.

2. Constraint equations between climbers and tether

In the current paper, the motion of the climbers along the tether is enforced by non-holonomic kinematic constraints [12, 21, 22]. As stated in the previous section, the climbers are assumed as lumped masses. Assuming there are m parallel tethers ($m \geq 2$), and each tether has w climbers ($w \geq 1$). The movement of climber is implemented by the moving nodes and variable-length elements. There are two steps to implement the movement of climber, (i) moving nodes with the time-varying material coordinate are assigned to the initial position of the climbers. (ii) adjacent elements connecting to the moving nodes are defined as the variable-length elements. The material coordinates of the moving nodes follow predefined trajectories of the climbers. Accordingly, constraint equations describing the motion of the climber are defined as,

$$C_{1,j}^{kl}(p,t) = \quad \left(k = 1,2,\ldots \quad \ldots \quad \text{or } \boldsymbol{C}_1(p,t) = \boldsymbol{0}\right. \tag{3}$$

where subscribe j denotes the node number of the moving node, superscripts k and l denote the index of climber and tether, respectively. $p_{j,\text{desired}}^{kl}$ denotes the pre-defined trajectory of the k^{th}

climber belong to l^{th} tether, the overhead dot represents the first order derivative with respect to time.

3. Constraint equations of normal nodes

Except for the moving nodes, the rest nodes are the normal nodes and their material coordinates are kept constant. Accordingly, the following constraint equations should be satisfied,

$$C_{2,k}\left(p,t\right)=\dot{} \qquad =1,j-1,j+1\ldots \qquad mw)\big) \text{ or } \boldsymbol{C}_2\left(p,t\right)=\boldsymbol{0} \tag{4}$$

4. Constraint equations of transverse support structure

As shown in Fig. 1, multiple parallel tethers are connected at end satellites by the transverse support structure with super high rigidity, for simplicity, the rigidity is assumed as infinite, the length is kept constant. The constraint equations of constant length are as,

$$\begin{cases} C_{3,1}=D_1^2-\left[\left(X_{1,j}-X_{1,k}\right)^2+\left(Y_{1,j}-Y_{1,k}\right)^2+\left(Z_{1,j}-Z_{1,k}\right)^2\right] \\ C_{3,2}=D_2^2-\left[\left(X_{\mathrm{n}+1,j}-X_{\mathrm{n}+1,k}\right)^2+\left(Y_{\mathrm{n}+1,j}-Y_{\mathrm{n}+1,k}\right)^2+\left(Z_{\mathrm{n}+1,j}-Z_{\mathrm{n}+1,k}\right)^2\right] \\ \begin{cases} j=1,2,\ldots \\ k=1,2,\ldots \\ j\neq k \qquad \end{cases} \end{cases} \text{ or } \boldsymbol{C}_3\left(p,t\right)=\boldsymbol{0} \tag{5}$$

where D_1^2 and D_2^2 are the square of constant distance connecting two tethers.

5. Equations of motion for the PSE with parallel multiple-tether and multiple-climbers

The equations of motion for the whole PSE can be obtained by combining Eqs. (2)-(5),

$$\begin{cases} \boldsymbol{M}_e\ddot{} \qquad \overline{j=1}\ \boldsymbol{\Im}_{j,X_e}^T\boldsymbol{\lambda}_j=\boldsymbol{F}_e+\boldsymbol{F}_g-\boldsymbol{F}_p \\ \boldsymbol{C}_1\left(p,t\right)=\boldsymbol{0} \\ \boldsymbol{C}_2\left(p,t\right)=\boldsymbol{0} \\ \boldsymbol{C}_3\left(p,t\right)=\boldsymbol{0} \end{cases} \tag{6}$$

where $\boldsymbol{C}_{j,\boldsymbol{X}_e}^T \left(j=1,2,3\right)$ denotes the Jacobian matrix of constraint equations with superscript T representing the transpose of matrix, and $\boldsymbol{\lambda}_j \left(j=1,2,3\right)$ denotes the vector of Lagrange multipliers corresponding to these constraint equations.

6. Merging and dividing of elements

The detailed information of the process of merging and dividing of element can be found in Refs. [10, 12, 13]. Here, only a brief introduction will be given. There are two types of elements are defined, the constant-length and variable length elements. The length of variable length element varies as the moving node (climber) moves along tether. To avoid its length excessively long or excessively short, special attention should be paid. Four parameters are defined to implement the process of dividing and merging of elements meanwhile suppresses the oscillation caused by the node removal. They are the standard element length L_s, the upper (L_{max}) and lower (L_{min}) bounds of an element length, and the acceptance criteria δ_e. These detailed parameters will be given in the simulation part.

C. Libration motion of PSE with parallel tethers

As shown in Fig. 3, the libration motion of the PSE can be easily expressed in the orbital coordinate system [1, 2, 6, 7, 23]. The detail definition of orbital coordinate system ($O'X_oY_oZ_o$) and transformation matrix from global coordinate system to the orbital coordinate system can be found in our previous work [13, 24]. The results of PSE are shown in the orbital coordinate system relative to the origin point. The libration motion of PSE with single tether cannot be directly used [6, 7, 13]. For the PSE with parallel tethers, the libration motion of PSE is defined as follows, a series of virtual libration angels are defined by straight lines connecting the main satellite, the

climbers, and the sub satellite, see the red dotted lines in Fig. 3. Taking the case of two climber and two parallel tethers as an example, there are six dotted lines. The in-plane angles $\alpha_{i,j}\left(i=1,\ldots \quad =1,2\right)$ and out-of-plane angles $\beta_{i,j}\left(i=1,\ldots \quad =1,2\right)$ are calculated as,

$$\begin{aligned}\alpha_{i,j} &= \tan^{-1}\left(\boldsymbol{R}_{X_o,i,j}/\boldsymbol{R}_{Z_o,i,j}\right),\\ \beta_{i,j} &= \tan^{-1}\left[-\boldsymbol{R}_{Y_o,i,j}/(\boldsymbol{R}_{Z_o,i,j}\cos\alpha_{i,j}+\boldsymbol{R}_{X_o,i,j}\sin\alpha_{i,j})\right]\end{aligned} \tag{7}$$

where $\boldsymbol{R}_{i,j}=\left(\boldsymbol{R}_{X_o,i,j},\boldsymbol{R}_{Y_o,i,j},\boldsymbol{R}_{Z_o,i,j}\right)^T$ is the vector of a dotted line expressed in the orbital coordinate system with the subscript $i\left(1\sim \quad\right.$ representing the sequence of these three lines belong to the j[th] $\left(1\sim \quad\right.$ tether.

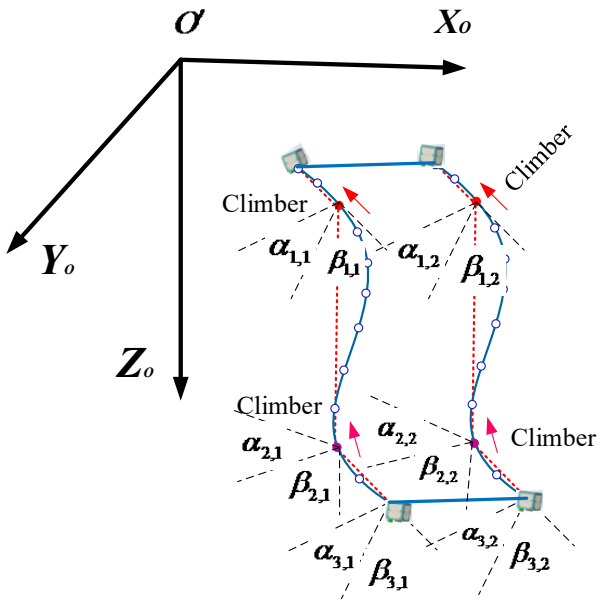

Fig. 2 Definition of libration angles of PSE with parallel tethers and multiple climbers.

III. Results and Discussion

In current paper, the Backward Euler formulation is employed together with the Newton-Raphson iteration method to solve this nonlinear differential algebraic equation (6) [12, 13, 25]. Among it, the maximum iteration number and error tolerance of each iteration step are set as 100 and 10^{-11},

respectively. For simplicity, the PSE is assumed to have two tethers, and the physical properties of the tether material of PSE are listed in Table.1, and other parameters will be given in the simulation part.

Table 1 Physical properties of tether

Parameters	Values
Number of parallel tethers	2
Material density of tether (kg/m^3)	1440
Elastic modulus of the tether ($10^9 N/m^2$)	72
Cross-section area (m^2)	2.0×10^{-6}

Table 2 Cases with simultaneous movement of climbers

Name	Motion of climber (Tether 1)	Motion of climber (Tether 2)
Case A	Upward	Upward
Case B	Downward	Downward
Case C	Upward	Downward
Case D	Downward	Upward

A. Effect of parallel tethers

In this section, the effect of parallel tethers influencing on the dynamic response of PSE is investigated. The numerical simulations are carried out at two scenarios, where climbers are supposed to move simultaneously in the first scenario and climbers are supposed to move with a time delay in the second scenario. Each tether has one climber only, and the climber is assumed to move along the tether at a constant speed 50 m/s. The PSE is assumed orbiting the Earth in a circular orbit initially, and the altitude of center of mass of PSE is 43164 km. The climber is supposed to move from a rest situation instantly, where the libration angle and velocity are zero. The physical parameters of PSE are used, L = 1000 km, $m_m = 10^7\ kg$, $m_s = 10000\ kg$, $m_c = 1500\ kg$. As listed in Table 2, both upward and downward transfer motions of climbers are

considered. The initial position of climber is locating $0.10L$ away from the end spacecraft. In this section, each tether is discretized into two variable-length elements without consideration of adding and subtracting of nodes, which leads the degrees-of-freedom of the PSE model is constant. The numbering of element starts from left tether to right tether, and it starts from up to upper to bottom in each tether. The element is counting consecutively. The time-step size is 0.001 s.

In the first scenario, four cases are carried out as listed in Table 2, where all the climbers move simultaneously. To investigate the effect of parallel tethers influencing the dynamic response of PSE, the results of PSE with parallel tethers are compared with results of PSE with a single tether. First, the comparison results for cases A and B are shown in Fig. 4-5 and Figs. 6-7, respectively. It can be easily found that the libration angles of the comparison results match very well as expected. It shows the difference of libration angles between the parallel-tether and single tether can be ignored when the climber's trajectories are the same. Furthermore, the same tendency of the variation of geometrical configuration of PSE is observed, seen Figs. 5 and 7. Second, the comparison results for cases C and D are shown in Figs.8-9 and Figs. 10-11. A significant difference is observed from the results of PSE with parallel tether comparing with the results of single tether when the movement directions of two climbers of each tether are opposite. For example, as shown in Figs. 8 and 10, the difference in the libration angles increases dramatically as times going on. Two reasons can be attributed, (i) the Coriolis forces of moving climbers are opposite (ii) the reaction forces caused by the rigid structure connecting two tethers. For example, as shown in Figs. 8 and 11, the variation of tension of PSE with transverse connecting structure varies different from the results of single tether. Because the two tethers interact with each other through the connecting structure. The same phenomenon is found by observing geometrical configuration of PSE, see Figs. 9 and 11. For example, the distance between two parallel tethers

increases for case C. however, for the case D, the distance decreases until two tethers tangle together. The tangling of two tethers should be stopped to happen from the design viewpoint. The reason is that the direction of Coriolis forces of two moving climbers is the same and point outward direction. For the case D, they are opposite and point inward direction. It reveals a fact, from the viewpoint of avoiding of tether collision, the movement direction of climber for PSE with parallel tethers is already determined once the rotational direction of PSE is determined. For example, the rotation axis of PSE is points to the positive Z-axis direction, the climber of left tether should be designed to move upward, and the climber of right tether should be designed to move downward.

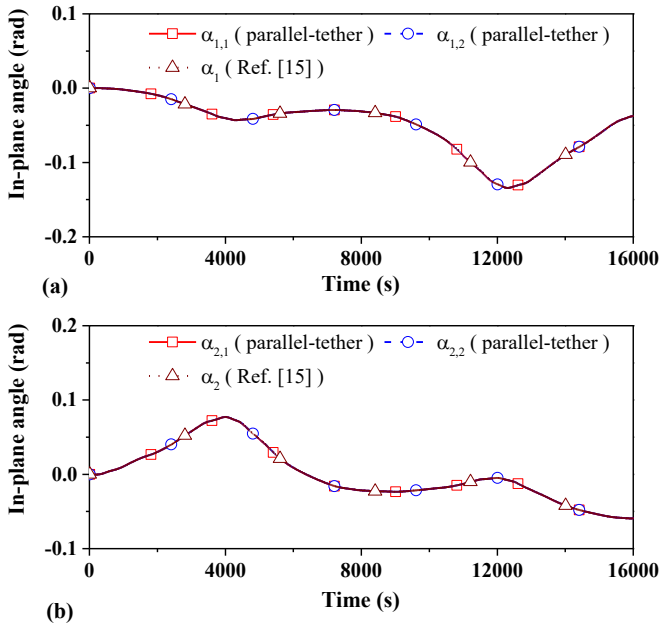

Fig. 3 Comparison results of libration angles of PSE in case A.

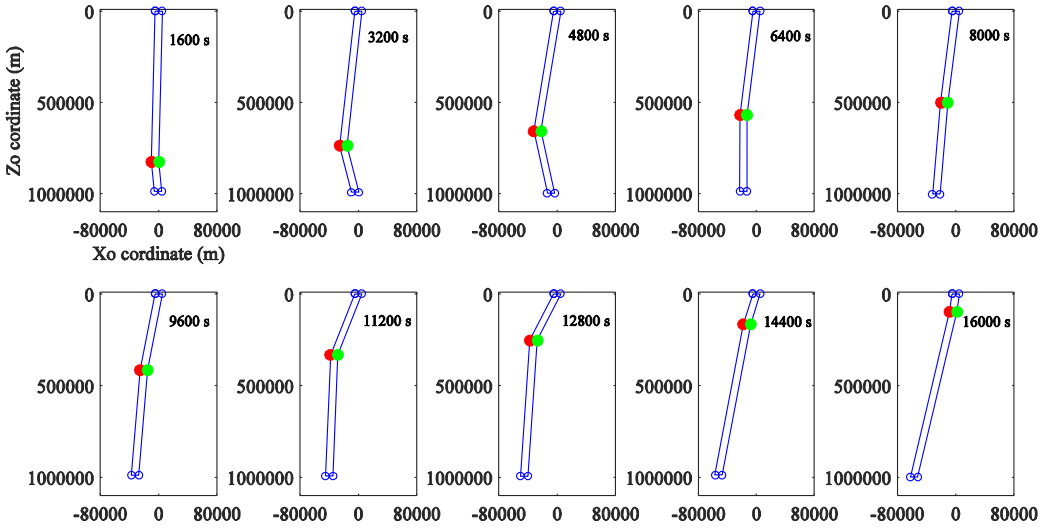

Fig. 4 Geometric configuration of PSE in case A

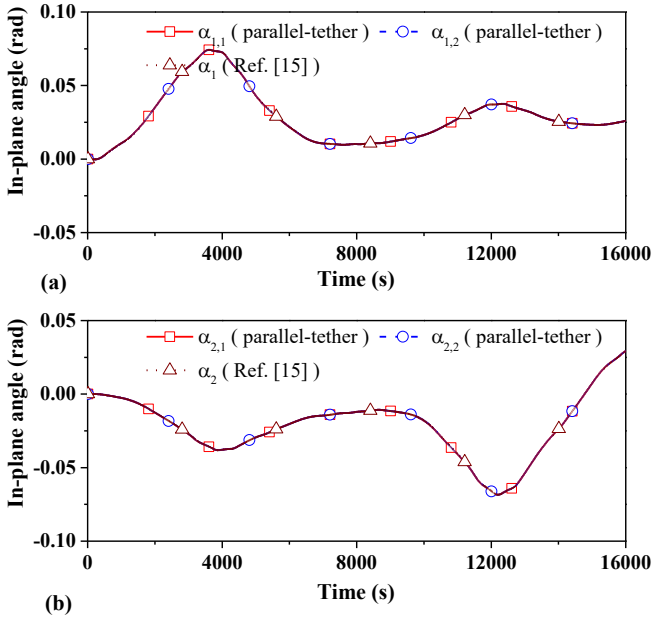

Fig. 5 Comparison results of libration angles of PSE in case B.

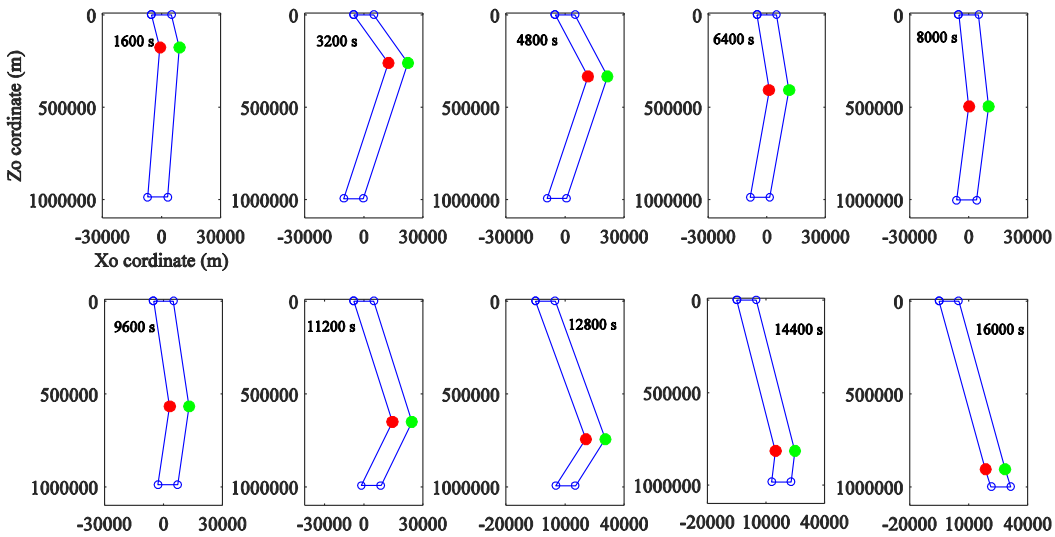

Fig. 6 Geometric configuration of PSE in case B.

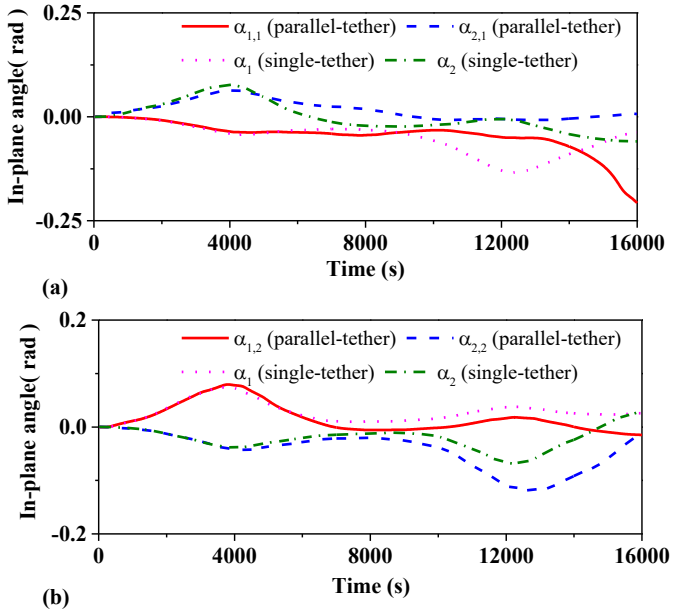

Fig. 7 Comparison results of libration angles of PSE in case C.

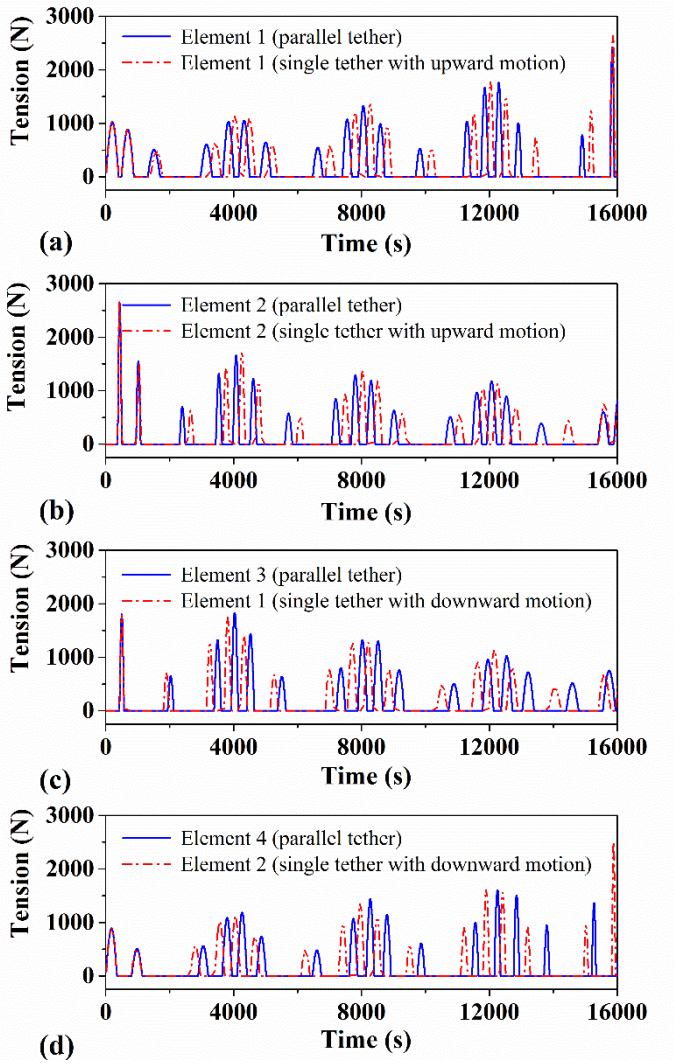

Fig. 8 Comparison results of tension in case C.

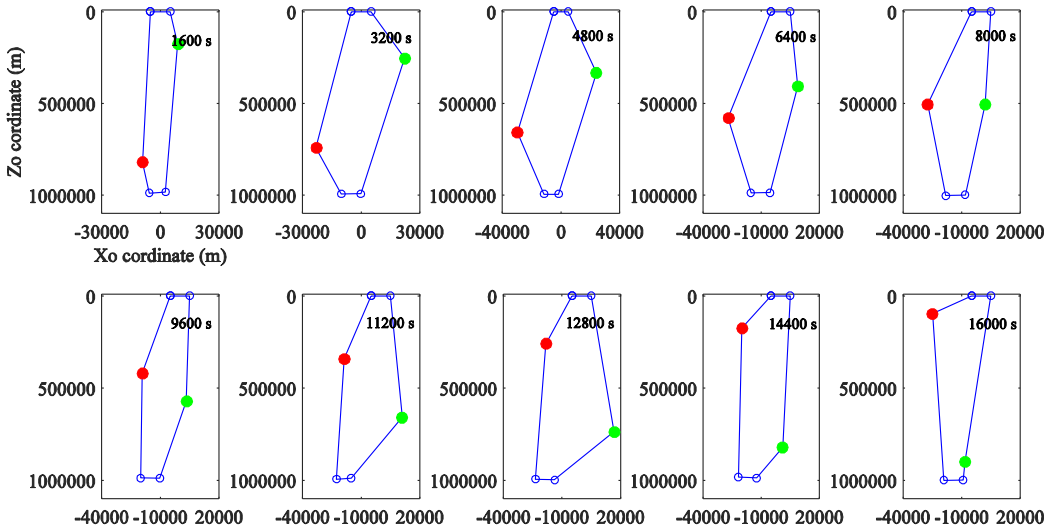

Fig. 9 Geometric configuration of PSE in case C.

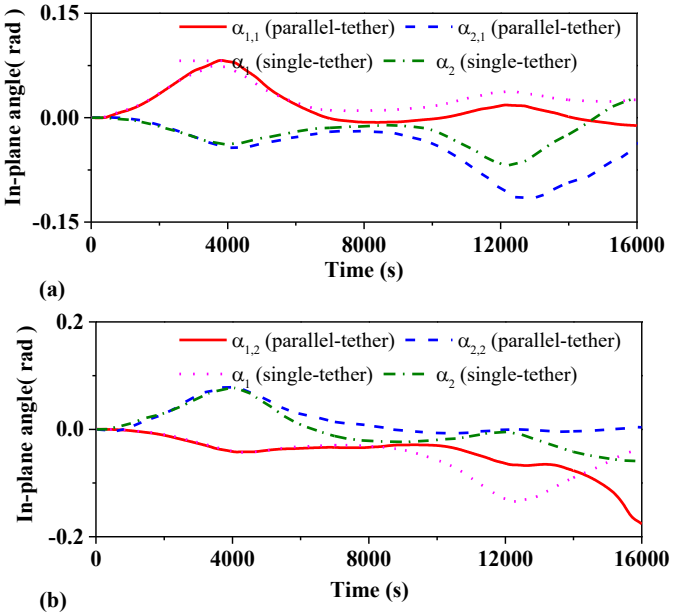

Fig. 10 Comparison results of libration angles of PSE in case D.

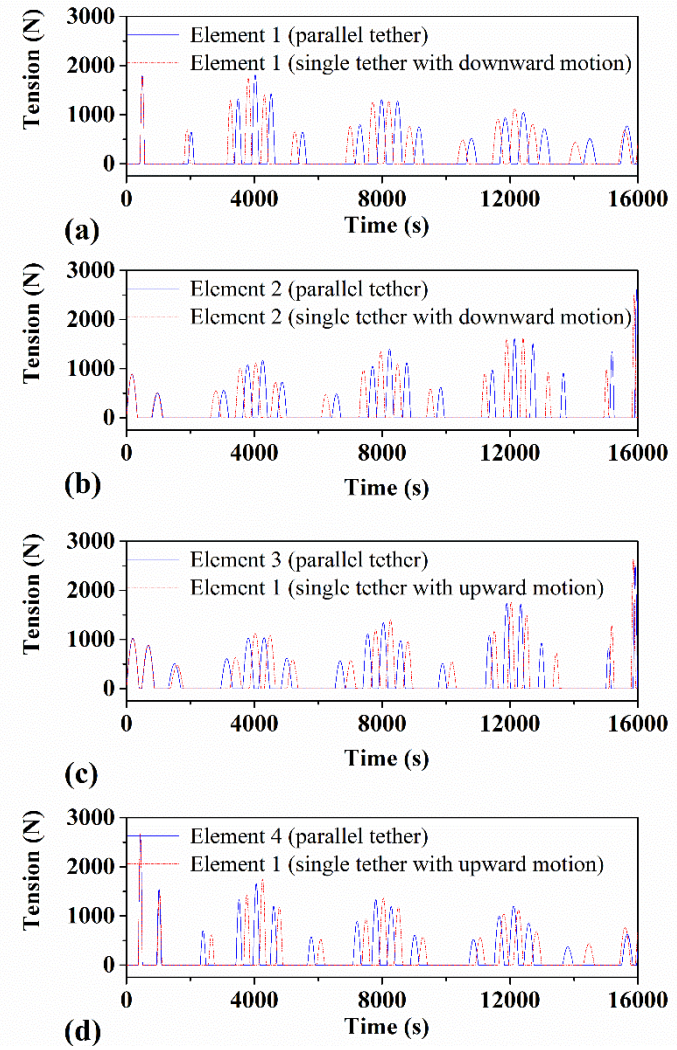

Fig. 11 Comparison results of tension in case D.

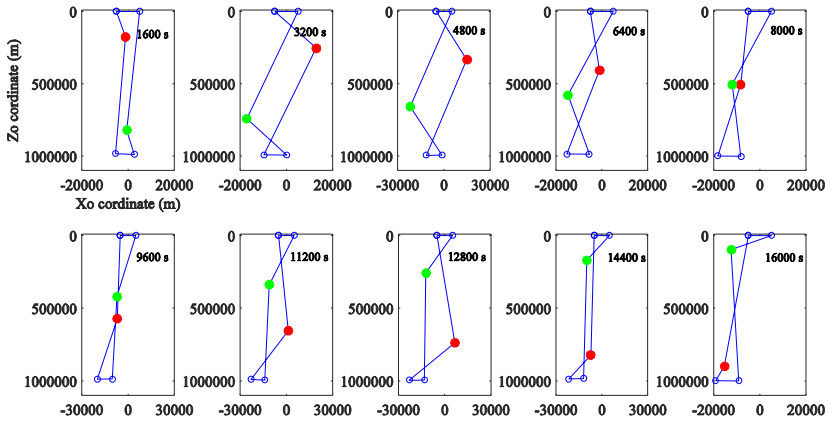

Fig. 12 Geometric configuration of PSE in case D.

In the second scenario, the climbers are supposed to move non-simultaneously. From simplicity, considering a time delay between climbers. As listed in Table 3, another three numerical simulations are carried out. For simplicity, the climber of left tether moves firstly, after 200 seconds, the climber of the second tether start to move. All the other parameters and initial conditions are the same as the cases A, B and C. The results are compared with the results of the cases A, B and C.

As shown in Fig. 13, the difference in the libration angles of PSE is not obvious at the start stage. However, the difference becomes noticeable as times going on. The same phenomenon can be observed from the geometric configuration of PSE as shown in Fig. 14. The reason for this phenomenon is that two tethers interact with each other caused by the non-simultaneously motions of climber.

In this section, we can conclude that dynamic behavior of PSE with parallel tethers is the same as the results of single tether when the motion of climber of each tether are the same. On the contrary, the noticeable difference in the dynamic behavior of PSE is found due to the interaction between two tethers when the motions of climber of each tether, including the movement direction and the time shift, are different.

Table 3 Cases with non-simultaneous movement of climbers

Name	Motion of climber (Tether 1)	Motion of climber (Tether 2)
Case E	Upward	Upward (200 s later)
Case F	Downward	Downward (200 s later)
Case G	Upward	Downward (200 s later)

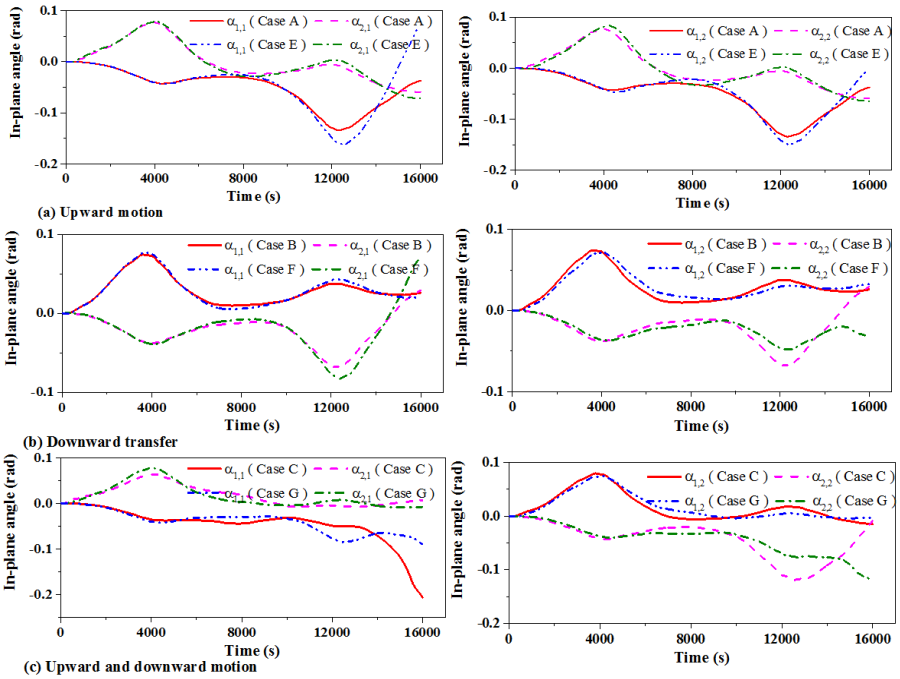

Fig. 13 Comparison results of libration angles of PSE considering time delay between two climbers.

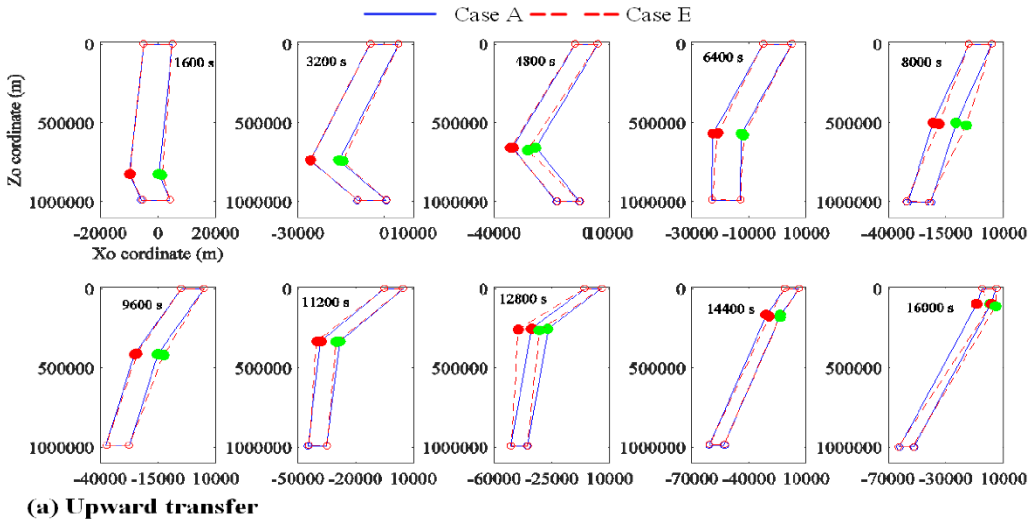

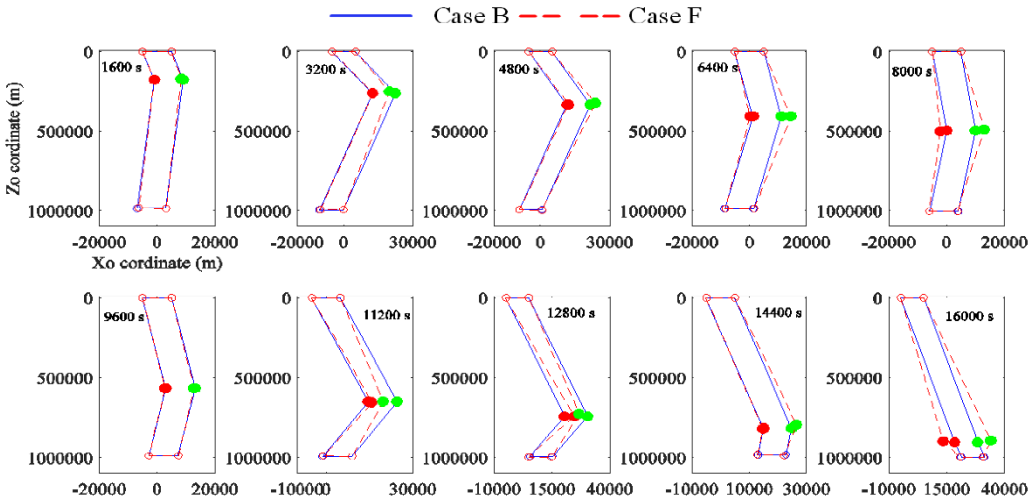

(b) Downward transfer

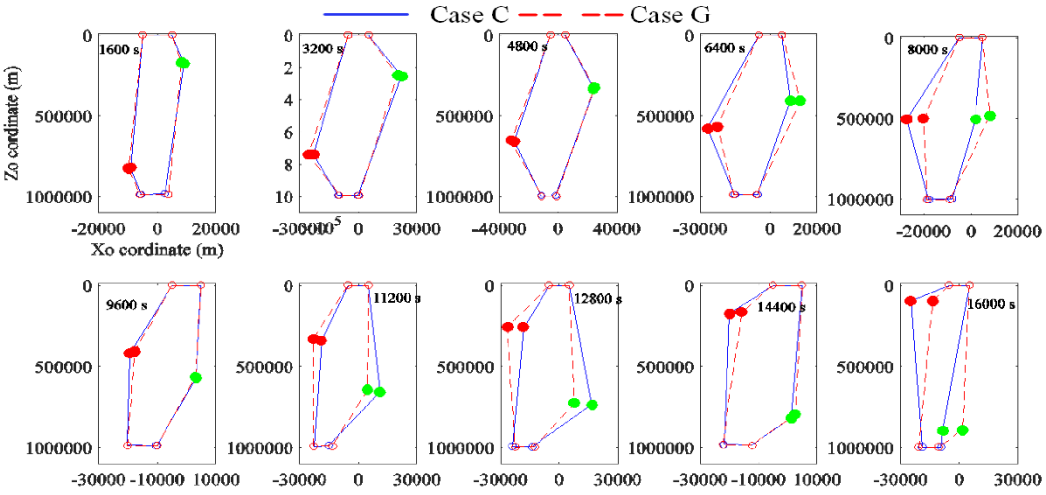

(c) Upward and downward transfer

Fig. 14 Comparison results of Geometric configuration of PSE considering time delay between two climbers

B. Effect of tether discretized scheme

In this section, the effect of tether discretization scheme on the dynamic response of PSE of parallel tethers is investigated. Here, each tether has one climber only, and the physical parameters, initial conditions, and motion of climber are set the same as Case C. As listed in Table 4, one tether was

discretized into two, four, six, eight, and twelve elements, and the other tether was discretized into the same element. Therefore, the total number of elements of PSE is double time of one tether. To observe the trend of convergence due to the discretization scheme, a new parameter is defined to show the difference in the position of climbers $R_{j,k} = \frac{\sqrt{\left(X_{c,k} - X_{c,j}\right)^2 + \left(Y_{c,k} - Y_{c,j}\right)^2 + \left(Z_{c,k} - Z_{c,j}\right)^2}}{\sqrt{X_{c,j}^2 + Y_{c,j}^2 + Z_{c,j}^2}} \times 100\%$ with subscripts j, k =4, 8, 12, 18, and 24 ($j \neq k$) representing the different discretization schemes of PSE.

First, the tethers are discretized into different element to investigate the effect of different discretization scheme, and the climbers are keeping still. The time step size is 0.001 s and the simulation time is 100 s. The results of the ratio $R_{j,k}$ are listed in Table 5. It can be easily seen that the difference in the ratio R decreases as the number of elements increases. For example, as listed in Table. 5, The $R_{16,24}$ is several times smaller than the $R_{4,8}$. However, the computational cost increases significantly for the Case J, however, the accuracy doesn't improve a lot. Thus, after the tradeoff analysis between the computational cost and accuracy, the PSE is discretized into sixteen elements with eight elements of each tether in the following simulations.

Second, as presented in section 2.7, the process of merging and dividing of elements occurs if the tether is discretized into more than two elements. Accordingly, the degree-of-freedom of the PSE model varies. For the PSE with parallel tethers, the setting of control parameters is different from the setting parameters of PSE with single tether [12, 13]. To avoid the processes of dividing and merging of elements of two tethers happen simultaneously, the standard length $L_{s,j}\left(j = 1,2\right)$ are chosen slightly different for two tethers. For the case J, $L_{s,1} = 12850\ m$ and $L_{s,1} = 15350\ m$, Other control parameters of the process of merging and dividing of element are set the same for

both two tethers, such as, $L_{max,j}=1.65L_{s,j}$, $L_{\min,j}=0.49L_{s,j}$, and $\delta_{e,j}=10^{-2}$ m ($j=1,2$). The comparison results of cases J and C are shown in Figs. 15 and 16. As shown in Fig. 15, it can be easily found the difference in the libration angles between Case C and Case J is obvious. Because the transverse motion of tether is included in the multiple elements tether model. The same phenomenon can be observed from the geometric configuration of PSE, see Fig. 16. It indicates the multiple elements tether model is more accurate to display the variation of PSE geometric configuration. Moreover, it is noticed that the two tether of PSE collides together that should be avoided. It indicates that the simultaneous optimization algorithm should be employed for the climbers to avoid the collision of tether.

In this section, it can be concluded that the tether model with multiple elements should be used to describe the geometrical configuration of PSE accurately, and the simultaneous optimization algorithm should be adopted to collision of tether.

Table 4 Number of elements of each tether

Name	Number of element (Left tether)	Number of element (Right tether)
Case H	4	4
Case I	6	6
Case J	8	8
Case K	10	10

Table 5. Ratio of position of climbers between different discretization schemes

Time (s)	Ratio $R_{4,8}$ (%) (climber 1)	Ratio $R_{8,12}$ (%) (climber 1)	Ratio $R_{12,16}$ (%) (climber 1)	Ratio $R_{16,24}$ (%) (climber 1)
10	4.38E-06	4.58E-07	1.21E-06	5.71E-08
20	1.69E-05	1.78E-06	8.22E-07	2.18E-07
30	3.69E-05	3.83E-06	2.43E-07	4.57E-07
40	6.33E-05	6.37E-06	4.57E-07	7.43E-07
50	9.44E-05	9.14E-06	1.20E-06	1.05E-06
60	1.28E-04	1.19E-05	1.92E-06	1.34E-06
70	1.63E-04	1.43E-05	2.57E-06	1.61E-06

80	1.96E-04	1.63E-05	3.09E-06	1.82E-06
90	2.26E-04	1.77E-05	3.48E-06	1.98E-06
100	2.51E-04	1.86E-05	3.73E-06	2.08E-06
Time (s)	**Ratio $R_{4,8}$ (%) (climber 2)**	**Ratio $R_{8,12}$ (%) (climber 2)**	**Ratio $R_{12,16}$ (%) (climber 2)**	**Ratio $R_{16,24}$ (%) (climber 2)**
10	3.71E-05	3.89E-06	1.32E-05	4.85E-07
20	1.50E-04	1.52E-05	1.65E-05	1.85E-06
30	3.31E-04	3.26E-05	2.14E-05	3.89E-06
40	5.70E-04	5.44E-05	2.74E-05	6.35E-06
50	8.55E-04	7.80E-05	3.38E-05	8.97E-06
60	1.17E-03	1.01E-04	4.01E-05	1.15E-05
70	1.50E-03	1.22E-04	4.56E-05	1.38E-05
80	1.81E-03	1.39E-04	5.01E-05	1.56E-05
90	2.10E-03	1.51E-04	5.32E-05	1.69E-05
100	2.34E-03	1.58E-04	5.48E-05	1.76E-05

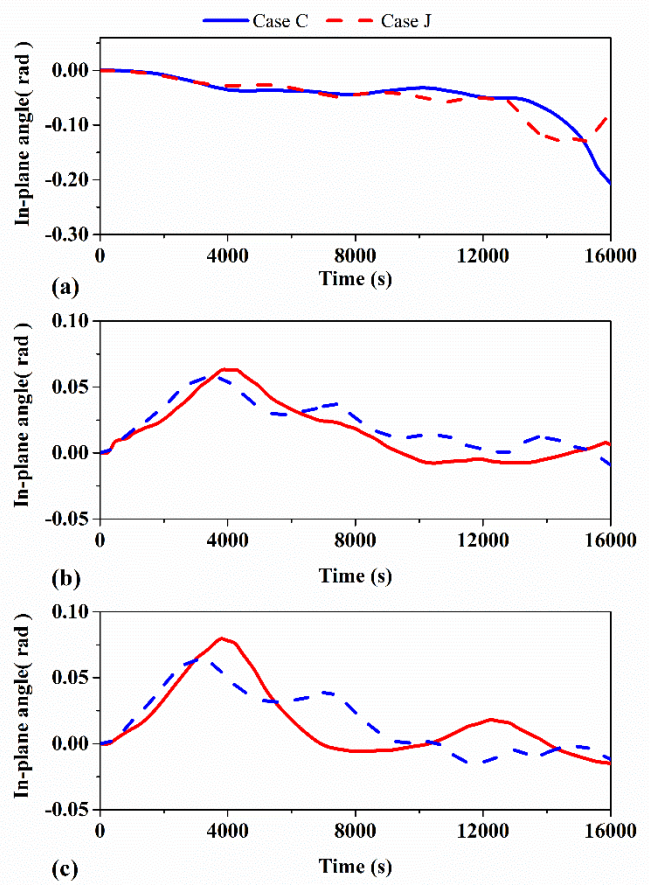

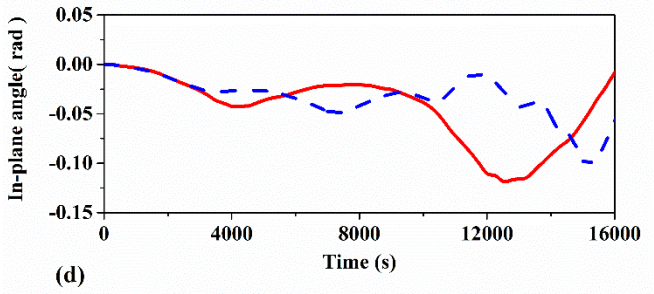

Fig. 15 Comparison results of libration angles of Case C and J (a) $\alpha_{1,1}$ (b) $\alpha_{2,1}$ (c) $\alpha_{1,2}$ (d) $\alpha_{2,2}$

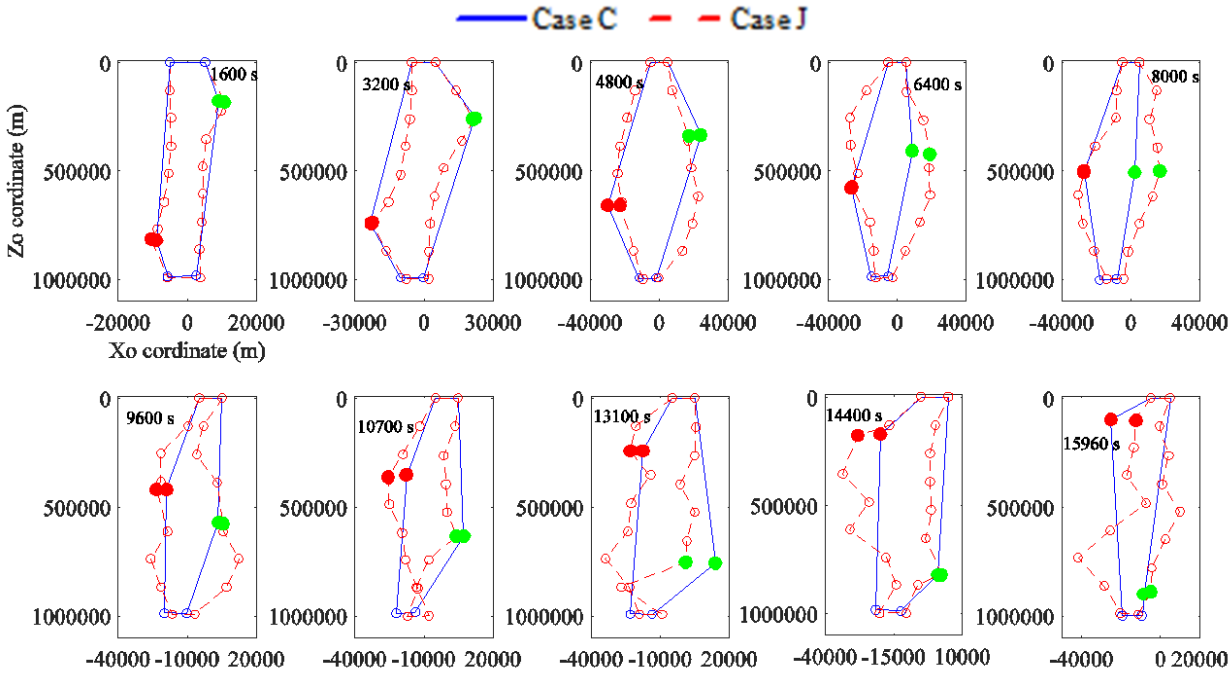

Fig. 16 Geometric configuration of PSE of Case C and J.

C. Effect of multiple climbers of each tether

In this section, the effect of multiple climbers influence on the dynamic response of PSE is investigated. The physical parameters, initial conditions, and the tether discretization scheme are set the same as in case J, except the parameters of climbers. One simulation case is conducted with each tether having two climbers with the same mass (half of mass of climber in Case J). As shown

in Fig. 17, the distance between two climbers of each tether is 10 km. The comparison results are shown in Figs. 18-20.

As shown in Figs. 18, it is easily found the difference in the libration angles between the comparison cases increases as the times going on. This is caused by the difference in the Coriolis forces of multiple climbers. As shown in Figs.18(a) and (d), it is seen that the amplitude of libration angle increases for the case J. It indicates the multiple climbers belong to each other without proper time shift may aggravate the libration motion of PSE. Therefore, the phase shift between each climber needs to be designed and optimized. For the case L, there is a high frequency of oscillation motion caused by the short distance between climbers, see Fig. 18(e). The same phenomenon can be observed from the geometrical configuration of PSE. Moreover, as shown in Fig. 19, it is found that the two tethers collide each other. It shows the control strategy needs to be explored to avoid the collision of tethers.

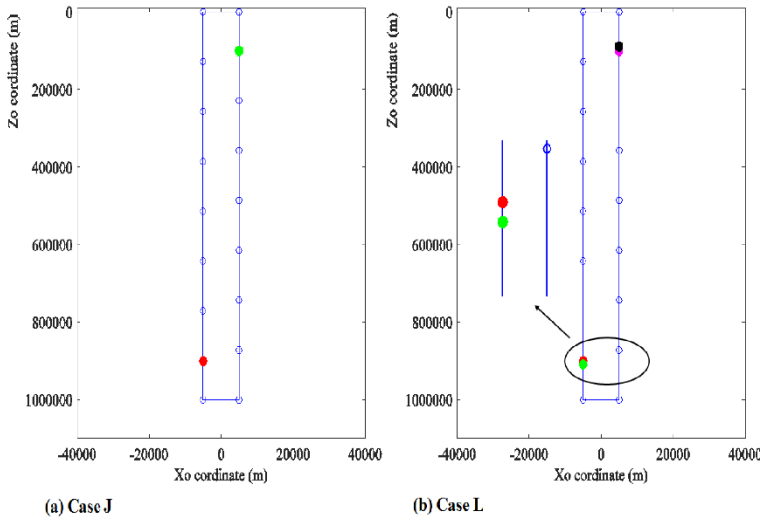

Fig. 17 The initial mesh of PSE between Case J and Case L.

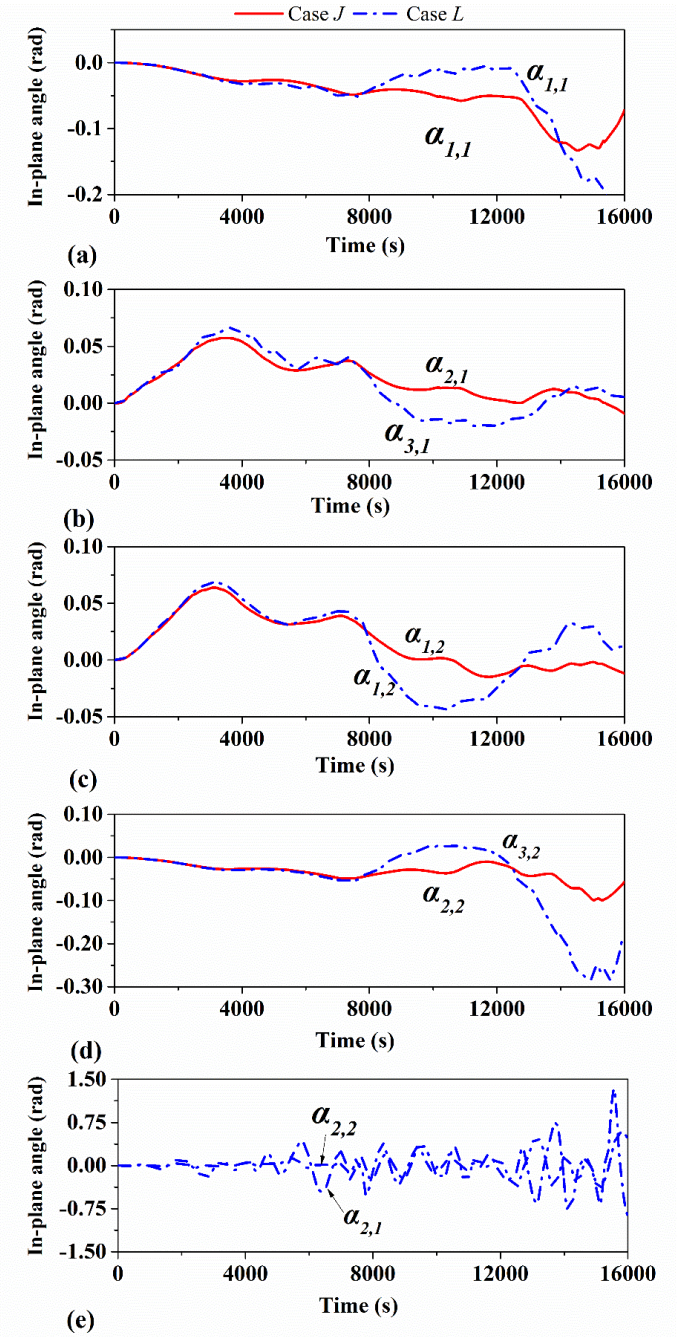

Fig. 18 Comparison results of libration angles of PSE in Cases J and L.

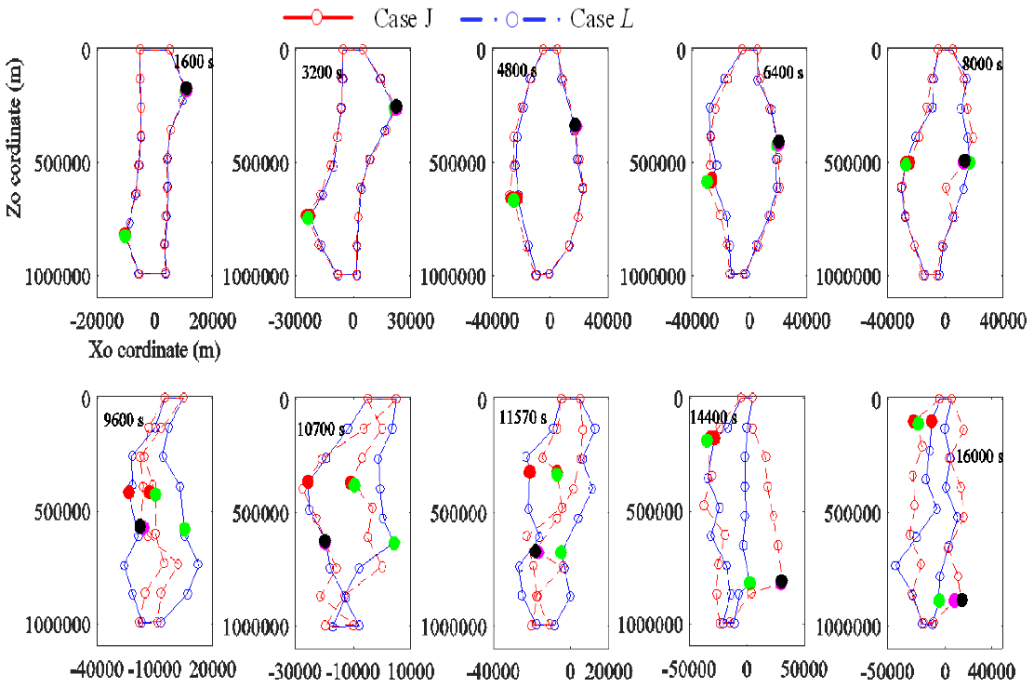

Fig. 19 Comparison results of Geometric configuration of PSE in Cases J and L.

IV. Conclusion

A novel concept of partial space elevator with parallel tethers and multiple climbers is proposed to increase the payload transfer efficiency. A high-fidelity and high-accuracy model of partial space elevator with parallel tethers is developed by the nodal position finite element method in framework of arbitrary Lagrangian-Eulerian. First, the concept of parallel tethers impacting on the dynamic response of PSE is investigated through the transient motion of climbers, the movement direction and time delay between climber. It is found that the tethers collide each other when the movement direction of climber is opposite. Therefore, for the safety operation of PSE with parallel tethers, the trajectories of climbers should be optimized to avoid the collision of tether. Second, the transient motion of multiple climbers of each other impacting on the dynamic response of PSE is studied, it is also found the tethers collide each other. Moreover, it is found the

multiple climber may aggravate the libration motion when the time shift between each climber is not well designed.

Acknowledgements

This work is supported by Discovery Grant (RGPIN-2018-05991) and Discovery Accelerate Supplement Grant (RGPAS-2018-522709) of Natural Sciences and Engineering Research Council of Canada.

References

[1] P. Woo, A.K. Misra, Energy considerations in the partial space elevator, Acta Astronautica, 99 (2014) 78-84.

[2] P. Woo, A.K. Misra, Dynamics of a partial space elevator with multiple climbers, Acta Astronautica, 67 (2010) 753-763.

[3] J.M. Knapman, P.A. Swan, Design concepts for the first 40km a key step for the space elevator, Acta Astronautica, 104 (2014) 526-530.

[4] E.C. Lorenzini, A three-mass tethered system for micro-g/variable-g applications, Journal of Guidance, Control, and Dynamics, 10 (1987) 242-249.

[5] E.C. Lorenzini, M. Cosmo, S. Vetrella, A. Moccia, Dynamics and control of the tether elevator/crawler system, Journal of Guidance, Control, and Dynamics, 12 (1989) 404-411.

[6] W. Jung, A.P. Mazzoleni, J. Chung, Dynamic analysis of a tethered satellite system with a moving mass, Nonlinear Dynamics, 75 (2014) 267-281.

[7] G. Shi, Z. Zhu, Z.H. Zhu, Libration suppression of tethered space system with a moving climber in circular orbit, Nonlinear Dynamics, 91 (2018) 923-937.

[8] X. Sun, M. Xu, R. Zhong, Dynamic analysis of the tether transportation system using absolute nodal coordinate formulation, Acta Astronautica, 139 (2017).

[9] P. Williams, W. Ockels, Climber motion optimization for the tethered space elevator, Acta Astronautica, 66 (2010) 1458-1467.

[10] G. Shi, G. Li, Z. Zhu, Z.H. Zhu, A virtual experiment for partial space elevator using a novel high-fidelity FE model, Nonlinear Dynamics, 95 (2019) 2717-2727.

[11] G. Shi, Z. Zhu, Z.H. Zhu, Stable orbital transfer of partial space elevator by tether deployment and retrieval, Acta Astronautica, 152 (2018).

[12] G. Li, Z.H. Zhu, On libration suppression of partial space elevator with a moving climber, Nonlinear Dynamics, (2019).

[13] G. Li, G. Shi, Z.H. Zhu, Three-Dimensional High-Fidelity Dynamic Modeling of Tether Transportation System with Multiple Climbers, Journal of Guidance, Control, and Dynamics, 0 (2019) 1-15.

[14] Y. Ishikawa, K. Otsuka, Y. Yamagiwa, H. Doi, Effects of ascending and descending climbers on space elevator cable dynamics, Acta Astronautica, 145 (2018) 165-173.

[15] G. Shi, G. Li, Z. Zhu, Z.H. Zhu, Dynamics and operation optimization of partial space elevator with multiple climbers, Advances in Space Research, 63 (2019) 3213-3222.

[16] G. Li, Z.H. Zhu, Precise Analysis of Deorbiting by Electrodynamic Tethers Using Coupled Multiphysics Finite Elements, Journal of Guidance, Control, and Dynamics, 40 (2017) 3348-3357.

[17] G.Q. Li, Z.H. Zhu, Long-term dynamic modeling of tethered spacecraft using nodal position finite element method and symplectic integration, Celestial Mechanics and Dynamical Astronomy, 123 (2015) 363-386.

[18] F.J. Sun, Z.H. Zhu, M. LaRosa, Dynamic modeling of cable towed body using nodal position finite element method, Ocean Engineering, 38 (2011) 529-540.

[19] S. Yang, Z. Deng, J. Sun, Y. Zhao, S. Jiang, A Variable-Length Beam Element Incorporating the Effect of Spinning, Latin American Journal of Solids and Structures, 14 (2017) 1506-1528.

[20] J.-P. Liu, Z.-B. Cheng, G.-X. Ren, An Arbitrary Lagrangian–Eulerian formulation of a geometrically exact Timoshenko beam running through a tube, Acta Mechanica, 229 (2018) 3161–3188.

[21] D. Hong, J. Tang, G. Ren, Dynamic modeling of mass-flowing linear medium with large amplitude displacement and rotation, Journal of Fluids and Structures, 27 (2011) 1137-1148.

[22] P. Williams, Dynamic multibody modeling for tethered space elevators, Acta Astronautica, 65 (2009) 399-422.

[23] S.S. Cohen, A.K. Misra, The effect of climber transit on the space elevator dynamics, Acta Astronautica, 64 (2009) 538-553.

[24] G. Li, Z.H. Zhu, J. Cain, F. Newland, A. Czekanski, Libration Control of Bare Electrodynamic Tethers Considering Elastic–Thermal–Electrical Coupling, Journal of Guidance, Control, and Dynamics, 39 (2015) 642-654.

[25] D. Hong, G. Ren, A modeling of sliding joint on one-dimensional flexible medium, Multibody System Dynamics, 26 (2011) 91-106.